HHS Public Access

Author manuscript

Neurobiol Dis. Author manuscript; available in PMC 2023 November 02.

Published in final edited form as:

Neurobiol Dis. 2023 October 15; 187: 106288. doi:10.1016/j.nbd.2023.106288.

Elevated susceptibility to exogenous seizure triggers and impaired interneuron excitability in a mouse model of Leigh syndrome epilepsy

Arena Manning[a,b], **Victor Han**[b], **Alexa Stephens**[b], **Rose Wang**[b], **Nicholas Bush**[b], **Michelle Bard**[b], **Jan M. Ramirez**[a,b,c], **Franck Kalume**[a,b,c,*]

[a]Graduate Program in Neuroscience, University of Washington, Seattle, WA, United States of America

[b]Center for Integrative Brain Research, Seattle Children's Research Institute, Seattle, WA, United States of America

[c]Department of Neurological Surgery, University of Washington, Seattle, WA, United States of America

Abstract

Mutations in the NADH dehydrogenase (ubiquinone reductase) iron-sulfur protein 4 (*NDUFS4*) gene, which encodes for a key structural subunit of the OXFOS complex I (CI), lead to the most common form of mitochondrial disease in children known as Leigh syndrome (LS). As in other mitochondrial diseases, epileptic seizures constitute one of the most significant clinical features of LS. These seizures are often very difficult to treat and are a sign of poor disease prognosis. Mice with whole-body *Ndufs4* KO are a well-validated model of LS; they exhibit epilepsy and several other clinical features of LS. We have previously shown that mice with *Ndufs4* KO in only GABAergic interneurons (Gad2-*Ndufs4*-KO) reproduce the severe epilepsy phenotype observed in the global KO mice. This observation indicated that these mice represent an excellent model of LS epilepsy isolated from other clinical manifestations of the disease. To further characterize this epilepsy phenotype, we investigated seizure susceptibility to selected exogenous seizure triggers in Gad2-*Ndufs4*-KO mice. Then, using electrophysiology, imaging, and immunohistochemistry, we studied the cellular, physiological, and neuroanatomical consequences of *Ndufs4* KO in GABAergic interneurons. Homozygous KO of *Ndufs4* in GABAergic interneurons leads to a

*Corresponding author at: Seattle Children's Research Institute, CIBR, JMB-10, 1900 Ninth Ave, Seattle, WA 98101, United States of America. fkalume@uw.edu (F. Kalume).

CRediT authorship contribution statement

Arena Manning: Conceptualization, Methodology, Investigation, Formal analysis, Visualization, Writing – original draft. **Victor Han:** Methodology, Investigation, Formal analysis. **Alexa Stephens:** Methodology, Investigation. **Rose Wang:** Conceptualization, Methodology, Investigation. **Nicholas Bush:** Formal analysis. **Michelle Bard:** Resources, Methodology, Investigation. **Jan M. Ramirez:** Resources, Funding acquisition, Methodology, Conceptualization, Supervision, Visualization. **Franck Kalume:** Resources, Funding acquisition, Methodology, Investigation, Conceptualization, Supervision, Visualization, Formal analysis, Writing – original draft, Writing – review & editing, Project administration, Validation, Data curation.

Declaration of Competing Interest

None.

Appendix A. Supplementary data

Supplementary data to this article can be found online at https://doi.org/10.1016/j.nbd.2023.106288.

prominent susceptibility to exogenous seizure triggers, impaired interneuron excitability and interneuron loss. Finally, we found that the hippocampus and cortex participate in the generation of seizure activity in Gad2-*Ndufs4*-KO mice. These findings further define the LS epilepsy phenotype and provide important insights into the cellular mechanisms underlying epilepsy in LS and other mitochondrial diseases.

Keywords

Epilepsy; Seizures; GABAergic interneuron; *Ndufs4* ; Excitability; hippocampus

1. Introduction

Leigh syndrome (LS), or subacute necrotizing encephalomyelopathy, is a progressive mitochondrial disease that primarily affects the central nervous system. It is the most common pediatric mitochondrial disease with an incidence of 1 in 40,000 live births (Rahman et al., 1996). Mutations in at least 75 different genes of both nuclear and mitochondrial genomes have been linked to LS (Lake et al., 2016). They represent defects in genes that encode proteins within the mitochondrial respiratory chain which drives oxidative phosphorylation (OXPHOS). The OXPHOS system comprises five multi-subunit protein complexes and among them the largest and most intricate is the Complex I (CI) which is composed of 44 subunits in mammals. CI plays an important role in energy metabolism; it serves as a main entry point for electrons into the mitochondrial respiratory chain. In particular, mutations in genes that encode all of CI subunits are known to cause LS and generally in its most severe form. One of these LS-causing CI genes is the *Ndufs4* gene, which codes for a subunit that is important for the structure and stability of the complex (Calvaruso et al., 2012; Ortigoza-Escobar et al., 2016).

Like most mitochondrial disorders, LS is clinically characterized by a set of multiple and highly variable symptoms. This includes seizures, ataxia, failure to thrive, hypotonia, psychomotor regression, breathing difficulties, dysphagia, cardiomyopathy, lactic acidosis, and premature death. The disease often presents within the first few months of life then quickly progresses to death by 2–3 years old (Rahman et al., 1996; van de Wal et al., 2022). However, adult-onset cases have also been reported (Piao et al., 2006; Bris et al., 2017).

Epileptic seizures are typically the first and one of the most dominant clinical manifestations of LS and other mitochondrial diseases. They have been reported to occur in 35–60% of patients with mitochondrial diseases (Rahman et al., 2012). In LS, this prevalence is estimated in the range of 40–79% (Rahman et al., 1996; Arii and Tanabe, 2000; Lee et al., 2009; Naess et al., 2009). These seizures are typically of multiple types including partial and/or myoclonic (MC) seizures, generalized tonic-clonic (GTC) seizures, as well as infantile spasms (Finsterer and Mahjoub, 2012). They are often resistant to standard antiepileptic drugs and thus are difficult to manage (Rahman and Copeland, 2019; Wesół-Kucharska et al., 2021). Furthermore, these seizures often significantly contribute to the deterioration of patients' cognitive function and lead to epileptic encephalopathy. As such, they profoundly affect the patients' prognosis and quality of life. However, despite their

major clinical significance, the pathophysiological mechanisms of seizures in the context of LS or other mitochondrial diseases are still not fully understood.

Our recent work showed that in LS, epilepsy is driven by GABAergic interneurons. Targeted knock-out (KO) of *Ndufs4* in only GABAergic (not glutamatergic) neurons was sufficient to recapitulate the severe and lethal epilepsy of LS in mice (Bolea et al., 2019). Mice carrying this type of mutation exhibited spontaneous interictal spikes, MC seizures, GTC seizures, and succumbed to sudden unexpected death in epilepsy (SUDEP) (Bolea et al., 2019). These mice were also sensitive to thermally induced MC and GTC seizures. Administration of selected standard antiepileptic drugs failed to ameliorate the seizures or prolong lifespan, illustrating resistance to standard epilepsy treatment (Bolea et al., 2019). These findings indicate that epilepsy can be reliably segregated and modeled away from other clinical manifestations of LS in Gad2-*Ndufs4*-KO mice. Therefore, these mice can be leveraged to specifically study the GABAergic mechanisms of epilepsy without the confounding factors of other LS symptoms and mechanisms.

In this study, to expand our understanding of the characteristics of epilepsy in LS, we examined the susceptibility of our mouse model to selected seizure triggers. People with epilepsy exhibit a high susceptibility to different seizure triggers. The latter can influence the timing and occurrence of seizures (Balamurugan et al., 2013; Ge et al., 2022). Exercise can cause a transient decrease in the seizure threshold and trigger seizures in people with epilepsy (Balamurugan et al., 2013). We recently showed that moderate exercise provokes GTC seizures in global *Ndufs4* KO mice (Bornstein et al., 2022). Here we explored whether this seizure-related phenotypic trait is recapitulated in the Gad2-*Ndufs4*-KO mice. We also assessed the seizure-inducing properties of pentylenetetrazol (PTZ), a GABA-A receptor antagonist used at low dose. By inhibiting GABAergic inhibition, PTZ enables synchronization of forebrain networks (Van Erum et al., 2020). When administered at sub-convulsive doses, PTZ commonly leads to MC seizures or absence seizures, whereas at convulsive doses it induces GTC seizures in wildtype rodents (Erakovic et al., 2001; Eloqayli et al., 2003; Van Erum et al., 2020). Since the GABAergic network is already affected by the genetic mutation, we examined whether a second hit with a low dose PTZ will reveal an increased susceptibility to seizures in our mouse model. Furthermore, we investigated the cellular, pathophysiological and neuroanatomical mechanisms underlying seizures in LS. Overall, we show that the *Ndufs4* KO in GABAergic interneurons leads to an increased susceptibility to tested exogenous seizure triggers, impaired interneuron excitability, and interneuron loss in the hippocampus and cortex. These findings shed a light on how dysfunctions of GABAergic interneurons drive the epilepsy phenotype in LS.

2. Methods

2.1. Ethics statement and animal use

All experiments were approved by the Institutional Animal Care and Use Committee of Seattle Children's Research Institute (Seattle, WA) under protocol ACU000108 (PI-Kalume). Animal numbers for each dataset are stated in the associated figure legend.

2.2. Generation of mouse model

B6.129S4-*Ndufs4*^{tm1Rpa}/J (*Ndufs4*$^{lox/lox}$) mice (Stock: 026963) were originally obtained from the laboratory of Dr. Richard Palmiter at the University of Washington (Kruse et al., 2008) and subsequently generated by our group and collaborators (Quintana et al., 2010; Bolea et al., 2019). B6N.Cg-*Gad2*$^{tm2(cre)Zjh}$/J (*Gad2*$^{Cre/+}$) mice (Taniguchi et al., 2011) were obtained from Jackson Laboratory (Stock No: 028867) (Bar Harbor, ME). B6.Cg-*Gt(ROSA)26Sor*$^{tm14(CAG-tdTomato)Hze}$/J (*CAG*$^{floxStop-tdTomato}$) mice carrying two alleles of floxed "STOP" sequence, preventing expression of red fluorescent protein, Tdtomato (Lox-Stop-Lox-TdTomato), were obtained from Jackson Laboratory (Stock No: 007914). Male and female mice were used in all experiments. Sex and age of the animals are described in the associated figure legends. All mice were on a C57BL/6 J background after backcrossing for at least 10 generations.

To produce Gad2 mutant (GAD2 MUT) and control (CON) mice Ndufs4$^{lox/lox}$ mice were crossed with the Gad2 Cre driver line. Experimental Gad2 mutants were *Ndufs4*$^{lox/lox}$*: Gad2*$^{Cre/+}$ and controls were *Ndufs4*$^{lox/lox}$*: Gad2*$^{+/+}$. Double floxed mice (Ndufs4$^{lox/lox}$: Ai14$^{lox/lox}$) were generated to genetically label all GABAergic neurons with conditional deletion of *Ndufs4*. To produce Gad2Cre-specific *Ndufs4* KO mice (*Ndufs4*$^{lox/lox}$*: Ai14*$^{lox/+}$*: GadCre*$^{+/-}$) we crossed *Ndufs4*$^{lox/lox}$*: Ai14*$^{lox/lox}$ with *Ndufs4*$^{lox/+}$*: GadCre*$^{+/-}$ mice. To produce Gad2Cre-specfic *Ndufs4* control mice (*Ndufs4*$^{+/+}$*: Ai14*$^{lox/+}$*: GadCre*$^{+/-}$) we crossed *Ai14*$^{lox/lox}$ *with GadCre*$^{+/-}$ mice.

2.3. Pentylenetetrazol (PTZ) seizure test

Mice were subcutaneously injected with PTZ (Sigma), a GABA-A receptor antagonist, at a subconvulsive dose of 20 mg/kg body weight and digital videos of the mice were recorded for 30 min post-PTZ injection. Principle behavior recorded on video was binned for 10 s and scored using the Racine scale of seizure severity (1, mouth and facial movements; 2, head nodding; 3, truck/whole body jerks; 4, forelimb/hindlimb clonus; 5, jumping/falling with forelimb/hindlimb clonus) (Racine et al., 1972). Seizure scoring was conducted by an experimenter blind to the genotype of the animals until statistical analysis.

2.4. Thermal seizure induction

Thermal seizure induction assay as previously reported (Bolea et al., 2019; Oakley et al., 2009). Rectal thermometer probes (Physitemp RET-5, attached to Physitemp TCAT-2DF monitor/controller) were taped to the side of the recording chamber down to the level of the animal for close temperature monitoring. The chamber temperature was set to 34.0 °C for two minutes, increased to 34.5 °C for two minutes, then increased by 0.2 °C every two minutes until a generalized tonic-clonic (GTC) seizure occurred or 35.0 °C was reached. All GTC seizures occurred at or before this temperature across mutant groups. Immediately after a GTC seizure, the heat lamp was removed, and mice were placed on an ice pack, with a small fan placed above to cool down. Mice returned to their home cages once baseline temperatures were reached.

2.5. Treadmill exercise as a seizure-inducing manipulation

Mutant and Control groups were separated into two age groups: Young (P30–45) and Old (P46–60). Prior to the test, mice were acclimated for five minutes to the treadmill apparatus (Bioseb, Pinnellas Park, FL). The treadmill was positioned horizontally with multiple running lanes. During the seizure test, mice were exposed to four consecutive trials of a low-stress exercise paradigm. During each trial, the treadmill belt speed was gradually increased from 5 to 20 m/min in 10 min followed by a 5 min recovery period period prior to the start of the next trial or the end of the test. Mice were monitored throughout the assay for seizure incidence. Seizures were characterized as generalized tonic-clonic. Experimenter was blind to the genotype of the animals during testing.

2.6. Sample preparation and histochemical procedures

Mice were anesthetized with isoflurane and perfused intracardially with phosphate-buffered saline PBS, pH 7.4, followed by phosphate-buffered 4% paraformaldehyde (PFA), pH 7.4. Whole brains were removed and placed in cold 4% PFA for at least 24 h. Brains were serially sectioned with a free floating vibratome (Leica VT 1000 S). Serial 50 μm coronal sections were collected in 1× PBS.

For cell loss experiments, serial 50 μm sagittal and coronal sections were collected from separate cohorts. Coronal sections were collected according to the Paxinos & Franklin's Mouse Brain Atlas (Franklin and Paxinos, 2013), focusing on specific a priori Regions of Interests (ROIs) within each section. Across 4 brain sections we analyzed 30 different ROIs for cell loss experiments. Free-floating sections (coronal and sagittal) were mounted in aqueous mounting media, DAPI Fluoromount-G mounting medium (Southern Biotech), cover slipped, sealed, and stored at 4 °C protected from light until imaging.

For cell counting experiments, sagittal brain slices were taken at 5× magnification on an Olympus BX61VS Scanning microscope (Olympus Life Science Inc.) using Olympus OlyVIA 2.9 software. Coronal brain slices were taken at 10× magnification on a Zeiss LSM 710 Imager Z2 Laser Scanning Confocal microscope (Carl Zeiss Inc.) using Zen 2009 software. Coronal sections were used for analysis, resulting in images of 512 × 512 μm in physical area. Images were collected with 16 line averages. DAPI was excited with a 405 nm laser, emissions collected at 424–503 nm. Ai14 was excited with a 543 nm laser, emissions collected at 548–587 nm. For cell counting quantification, coronal images were analyzed using ImageJ/FIJI software (NIH, Bethesda, Maryland, USA).

For cFos experiments, serial 50 μm sagittal sections (two per animal) were washed thrice in PBS, rinsed in 0.5% Triton/PBS solution, then blocked in 10% serum in PBS with 0.5% Triton X-100, then incubated overnight at 4 °C with rabbit anti-c-fos (EMD Millipore) polyclonal primary antibody. The next day, sections were washed four times in PBS, incubated with goat anti-rabbit Alexa fluor plus 488 (Thermo Fisher Scientific) secondary antibody for 2 h at room temperature. Sections were mounted in an aqueous mounting media, DAPI Vectashield Antifading Mounting Medium (Fisher Scientific) to visualize nuclei. Immunostained sections were imaged with an Olympus BX61VS Scanning microscope (Olympus Life Science Inc.) using Olympus OlyVIA 2.9 software at 5×

magnification, then later processed using Image J software (NIH, Bethesda, Maryland, USA).

2.7. Electrophysiology

Mice were anesthetized with isoflurane, their brains quickly removed and sliced (350 μm thick; coronal plane) using the Leica VT1000S vibratome in ice-cold oxygenated (95% O_2, 5% CO_2, carbogen) slicing solution (in mM: KCl 5, NaH_2PO_4 1.25, $MgSO_4$ 3.5, $CaCl_2$ 0.5, $NaHCO_3$ 26, glucose 10, sucrose 210). After a 30-min incubation in oxygenated slicing solution, slices were transferred to a chamber with oxygenated artificial cerebrospinal fluid (ACSF, in mM: NaCl 118, KCl 3, $CaCl_2$ 1.5, $MgCl_2$ 1, $NaHCO_3$ 25, NaH_2PO_4 1, glucose 30). For at least 30 min, slices were allowed to equilibrate in ACSF at room temperature. Individual slices were transferred to the recording chamber and perfused with oxygenated ACSF at 3.2–3.8 ml/min flow rate.

Hippocampal CA1 Ai14-labeled interneurons were visualized using a differential interference contrast microscope. Whole-cell patch clamp recordings were carried out at room temperature using a MultiClamp 700B Amplifier (Axon Instruments) and digitized with a Digidata 1400 (Axon Instruments). Patch clamp experiments were performed using borosilicate glass capillaries pulled on Sutter Instruments P-97 puller. Patch pipettes had a resistance of 3 to 5 M Ohm. Patch-clamp currents were filtered at 2.1 kHz and sampled at 10 kHz. Cells were held at −80 mV. Firing patterns were recorded in response to prolonged depolarization and hyperpolarization currents (duration: 800 ms; increments, 10 pA). Extracellular recording solution contained oxygenated ACSF (in mM: NaCl 118, KCl 3, $CaCl_2$ 1.5, $MgCl_2$ 1, $NaHCO_3$ 25, NaH_2PO_4 1, glucose 30). The intracellular solution contained (in mM): KCl 135, HEPES 10, Mg-ATP 2, Na-GTP 0.2, EGTA 0.5; pH 7.4. We recorded the input-output relationship, action potential threshold, half-width, width and peak, minimum voltage, and input resistance. Input-output relationship was determined by the number of action potentials generated by the amplitude of current injection. The threshold was determined by the first action potential during depolarization as the voltage corresponding to the peak of the third differential of the action potential waveform. Action potential half-width was measured by halfheight and width by threshold. Input resistance was measured as the slope of the linear regression of the *I*-*V* plot for a series of hyperpolarizing pulses, where "*I*" was current amplitude and "*V*" was steady-state voltage.

2.8. Statistical analysis

Statistical significance was assessed using 2-tailed unpaired *t*-tests to determine if there were any statistically significant differences in the number of Ai14-labeled GABAergic interneuron cell bodies in each image between control and mutant mice for each ROI. No difference was found for female and male mice; thus, they were pooled for both groups. Each data point represents the number of cells/unit area for each mouse. Statistical significance was set at $p < 0.05$. Values are displayed as the mean ± SEM. Analysis was performed in GraphPad Prism v5.01 (GraphPad Software Inc., San Diego, USA).

3. Results

3.1. Homozygous KO of Ndufs4 in GABAergic interneurons leads to increased susceptibility to exogenous seizure triggers

We previously showed that Gad2-*Ndufs4*-KO mice exhibit thermally induced GTC seizures (Bolea et al., 2019). To further characterize epilepsy in these mice, we investigated their susceptibility to other exogenous seizure triggers. The mice were exposed to a low, subthreshold dose (20 mg/kg) of pentylenetetrazol (PTZ). Given that interneuron function is already impacted by a genetic lesion, we predicted a second hit of the GABAergic network by administration of a low dose of PTZ may be sufficient to provoke GTC seizures in the *Ndufs4*-related model of LS.

Gad2-*Ndufs4*-KO (n = 9) and control (n = 9) mice (P50–60) received a single sub-convulsant dose (20 mg/kg) of PTZ and were monitored for seizure behaviors (Methods). Following PTZ injection, the Gad2-*Ndufs4*-KO mice exhibited periods of immobility and overt convulsive activity marked by myoclonic (MC) seizures of Racine 2–3 severity that progressed into generalized tonic clonic (GTC) seizures of Racine 4–5 severity in a subset of the mice. In contrast, control mice showed only MC seizures ranging from Racine 2–3 severity; no GTC seizures or mortality were observed in this group (Fig. 1A, B, C). In addition, the frequency and time spent in the ictal stage were higher in the mutant compared to the control group (Supplementary Fig. 1A–C). Video-EEG-EMG studies showed that the behavioral outcomes of each PTZ-induced MC seizure correlated with a brief, fast spike- or polyspike-and-wave EEG discharge concurrent with a burst of high amplitude activity on EMG during a brief bilateral contraction of neck and body musculatures in both control and mutant mice. Further, PTZ–induced GTC seizures were characterized on their onset by bursts of generalized spikes of increasing amplitude and decreasing frequency coinciding with increased EMG activity during bilateral clonic jerks of extremities in only mutant mice. This initial ictal phase was ensued by high-amplitude spike-and-slow wave discharges associated with increased EMG activity during tonic contractions of the muscles. Post-ictally, both EEG and EMG signals showed a notable suppression of activity. (Fig. 1D–E). Mutants showed an increase in Racine 3–5 total percent time seizing (Fig. 1F). EEG spectrogram analysis showed a prominent increase in power across all frequency bands (0.5-60 Hz) during non-fatal and fatal GTC seizure events (red arrowheads) in Gad2-*Ndufs4*-KO mice (Fig. 1G). These findings suggest that a low dose of PTZ known to be sub-convulsive for WT mice, is sufficient to provoke GTC seizures in mice harboring *Ndufs4* KO in GABAergic neurons. These results also indicate that mutant mice show an increased susceptibility to GTC seizures when challenged with a pharmacological suppression of GABAergic network activity.

In further studies, we determined seizure susceptibility following a moderate exercise paradigm in our mice with LS-related epilepsy. Tests were conducted at early (P35–45) and late (P46–60) developmental points to determine phenotype progression. The results showed that both young and old mutants have a greater GTC seizure susceptibility compared to littermate controls (Fig. 1H). Importantly, convulsive seizures only occurred during the 5-min recovery periods between trials or after of the last trial of the test. These findings

suggest that KO of *Ndufs4* in GABAergic neurons alone is sufficient to render mice susceptible to exercise-induced.

3.2. Homozygous Ndufs4 KO leads to impaired excitability of GABAergic interneurons in mice

Knock out of *Ndufs4* leads to mitochondria dysfunction (Smeitink et al., 2001; Kruse et al., 2008). On its turn, mitochondrial dysfunction has been shown to alter cellular excitability (Kang et al., 2013; Kann et al., 2011; Whittaker et al., 2011). To examine the impact of the *Ndufs4* KO on the excitability of GABAergic neurons, we generated Gad2Cre-specific *Ndufs4* KO and control mice in which GABAergic interneurons were labeled with tdTomato (Methods). Whole-cell patch clamp recordings from P30–40 mice were obtained from CA1 hippocampal GABAergic neurons visually identified based on tdTomato fluorescence in brain slices (Supplementary Fig. 2A).

These recordings revealed that a large portion (60%) of Gad2-*Ndufs4*-KO CA1 GABAergic interneurons, referred to as the mutant impaired group (red), exhibited a biphasic impairment of action potential (AP) firing. In response to lower depolarization current injections (< 150 pA), these cells fired more actions potentials than their control (black) counterparts. Further increase in depolarizing current injections (> 150 pA) unveiled a dramatic failure in the ability of these cells to generate more action potentials and maintain a similar firing rate as control cells (Fig. 2A–B; Supplementary Fig. 2B). A smaller portion (40%) of mutant cells, called the mutant unimpaired group (purple), showed a similar firing response profile compared to control cells. These results show that the *Ndufs4* KO leads to a profound decrease of CA1 hippocampal interneuron excitability in Gad2-*Ndufs4*-KO mice.

Other assessments (Table 1; Fig. 2C–I) revealed that Gad2-*Ndufs4*-KO CA1 GABAergic interneurons exhibited several other changes in electrophysiological properties. Mutant impaired cells showed on one hand a decrease in capacitance, rheobase, and AP height compared to control cells, indicating that KO of *Ndufs4* reduces cell size, the minimal depolarization required for action potential generation, and the cell's ability to reach the higher peak of the action potential. On the other hand, these cells showed an increase in AP width, input resistance, and afterhyperpolarization (AHP), revealing the *Ndufs4* KO increases the time to complete an action potential and simultaneously lowers the membrane conductance and peak AHP potential of a cell. Surprisingly, mutant unimpaired cells also showed several electrophysiological changes. They exhibited an increase in AP height, AP width, and AHP height, indicating that the *Ndufs4* KO increases the ability to reach a higher AP peak and simultaneously decreases the time to complete an AP, and the AHP peak potential of a cell. These findings demonstrate that the *Ndufs4* KO impaired several cellular electrophysiological properties that contribute to neuronal excitability in CA1 hippocampal interneurons.

3.3. Homozygous Ndufs4 KO results in GABAergic interneuron loss in key regions associated with epilepsy

GABAergic interneurons are more vulnerable to mitochondria dysfunction (Lax et al., 2016). The later has been shown to impair interneuron migration during development (Lin-

Hendel et al., 2016). Furthermore, dysfunction or loss of GABAergic interneurons leads to seizures (Hunt and Baraban, 2015; Katsarou et al., 2017). We examined whether KO of *Ndufs4* leads to reduced GABAergic interneurons cell density in brain regions associated with epilepsy.

We crossed Gad2Cre-specific *Ndufs4* KO mice with a reporter mouse carrying tdTomato and examined the expression of fluorescently labeled GABAergic interneurons in mice aged P43–50 (Fig. 3A). Gad2-*Ndufs4*-KO mice showed a significant reduction in the number of Ai14 (red) expressing interneurons in the CA1 subfield (caudal) of the hippocampus compared to controls (GAD2 MUT: $N = 7$; CON: $N = 6$; GAD2 MUT mean ± SEM = 116.3 ± 12.9; CON mean ± SEM = 164.2 ± 9.4; two-tailed Student *t*-test, Welch correction, $P = 0.0144$), resulting in a 30% reduction of interneurons in this region (Fig. 3B). Mutants showed a significant reduction in the number of interneurons in the central amygdala (CeA) (GAD2 MUT: N = 7; CON: N = 6; GAD2 MUT mean ± SEM = 381.8 ± 52.3; CON mean ± SEM = 594.0 ± 67.6; two-tailed Student t-test, Welch correction, $P = 0.0311$) resulting in a 35% reduction in the number of interneurons in this region (Fig. 3C). Mutants also showed a significant reduction in the number of interneurons in the posteromedial cortical amygdala nucleus (PMCo) (GAD2 MUT: N = 7; CON: N = 6; GAD2 MUT mean ± SEM = 257.0 ± 32.9; CON mean ± SEM = 354.0 ± 27.2; two-tailed Student t-test, Welch correction, $P = 0.0458$), resulting in a 27% reduction in the number of interneurons in this region (Fig. 3D). Cell loss was not detected in hippocampal DG, CA1 rostral, and CA2/CA3 domains, nor across distinct cortical regions (Supplementary Fig. 3A–B).

We conclude that the *Ndufs4* KO in GABAergic interneurons causes a decrease in interneuron cell density in regions known to generate epilepsy.

3.4. Seizures are associated with increased activity in the hippocampus and cortex of Gad2 Ndufs4 KO mice

The hippocampus and cortex are known to participate in generalized tonic clonic seizures. To assess the involvement of these brain regions in spontaneous and provoked GTC seizures in Gad2-*Ndufs4*-KO mice, we used cFos immunoreactivity, a commonly used biochemical technique to visualize and map neuronal activity (Morgan et al., 1987; Herrera and Robertson, 1996).

Gad2-*Ndufs4*-KO and control mice (P55–60) were submitted to the protocol for thermal induction (TI) of seizures or to a sham protocol. Four experimental groups were generated based on genotype and seizure history: (1) Gad2-*Ndufs4*-KO TI (2) Gad2-*Ndufs4*-KO Sham (3) Gad2-*Ndufs4*-control TI (4) Gad2-Ndufs4-control Sham. Sagittal images of mice from Gad2-*Ndufs4*-KO TI and *Ndufs4*-control TI groups, showed cFos activated neurons (green) and all neurons (blue) across the brain (Fig. 4B). Gad2-*Ndufs4*-KO TI mice that were GTC responders showed an increase in cFos activity within the DG subfield of the hippocampus compared to *Ndufs4*-control Sham and Gad2-*Ndufs4*-KO Sham mice (Fig. 4C). To determine changes in neuronal activity in the frontal cortex, we counted the number of DAPI positive (blue) and cFos-positive (green) cells in this region. Gad2-*Ndufs4*-KO TI mice showed an increase in the number of cFos-positive cells compared to Gad2-*Ndufs4*-KO Sham and *Ndufs4*-control TI mice (Fig. 4D), with no change in the number of neurons

(Supplementary Fig. 4A) suggesting that the *Ndufs4* KO alters the number of activated cells and not pan neuronal cell density in the frontal cortex. These findings suggest that thermally induced seizures are associated with increase neuronal activity of the hippocampus and cortex of mice with *Ndufs4* KO..

Whether thermally induced and spontaneous seizure activity in Gad2-*Ndufs4*-KO mice engage the same brain regions is unknown. Therefore, we also evaluated changes in cFos activity in mutants following spontaneous seizures. Opportunistically, tests were conducted on mice that were observed to have spontaneous seizure during routine husbandry tasks. A mouse exhibiting spontaneous seizures that evolved into status epilepticus (S.E.) was identified and examined for cFos immunoreactivity. Results from this mouse and from TI and sham groups were compared. The mouse with spontaneous S.E. showed an increase in cFos activity within the DG compared to Gad2-*Ndufs4*-KO Sham mice, however, there was no difference in cFos activity between the S.E. mouse and Gad2-*Ndufs4*-KO TI mice (Supplementary Fig. 4B). These findings suggest that both spontaneous and thermally induced seizures in mice with the *Ndufs4* KO increase neuronal activity in the DG, a change that reliably correlates with seizure activity. Additionally, S.E. led to an increase in the number of cFos positive cells in the frontal cortex (Supplementary Fig. 4C) when compared to both Gad2-*Ndufs4*-KO Sham and Gad2-*Ndufs4*-KO TI mice.

These findings indicate that targeted *Ndufs4* KO in GABAergic interneurons causes an increase in cFos activity in the hippocampus and cortex in this model. This increase in cFos activity was associated with not only thermally induced seizures but also spontaneous seizures in the hippocampus and cortex, two regions associated with seizure generation.

4. Discussion

As in most mitochondrial diseases, epilepsy is a prominent feature among the multiple neurological phenotypes of LS. Epileptic seizures are often difficult to manage with standard antiepileptic drugs and they strongly affect the disease prognosis. In our recent work, we showed that Gad2-*Ndufs4*-KO exhibit a severe epilepsy phenotype, serving as an excellent preclinical model of LS-epilepsy. The pathophysiological mechanisms underlying LS-epilepsy are not fully understood. In this study, we show that an exogenous trigger such as a low dose of a pharmacological convulsant agent or moderate exercise, readily provokes GTC seizures in Gad2-*Ndufs4*-KO mice. We show that KO of *Ndufs4* has a direct negative impact on interneuron function and survival. Further, hippocampal and cortical neurons are key participants in the generation of spontaneous and provoked seizures in the mice carrying the *Ndufs4* KO in GABAergic interneurons.

4.1. Selected exogenous triggers precipitate seizures in Gad2-Ndufs4-KO mice

We have recently shown that GABAergic interneurons (not glutamatergic neurons) play a crucial role in LS-related epilepsy (Bolea et al., 2019). In this study, we showed that when challenged to a low dose of the proconvulsant, PTZ, Gad2-*Ndufs4*-KO mice exhibit a lower threshold for MC seizures, as well as GTC seizures compared to controls (Fig. 1). Additionally, GTC seizures immediately lead to mortality in about 20% of Gad2-*Ndufs4*-KO mice.

As noted above, a variety of endogenous and exogenous factors can precipitate seizures in people with epilepsy. PTZ is a proconvulsant that has been commonly used to generate mouse models of acute seizures or epilepsy (recurrent seizures) for preclinical research since the 1940s. These animal models have been very valuable for the discovery of several antiepileptic drugs currently on the market (Krall et al., 1978; Löscher, 2017). PTZ mechanisms of action is thought to be primarily caused via antagonistic effects on GABA-A receptors leading to suppression of inhibitory synapses and overall network hyperactivity. Consistent with our hypothesis that a second hit on the GABAergic network that is already weakened by the *Ndufs4* KO will readily provoke seizures in mice, our results demonstrate that a low-dose PTZ-mediated suppression of GABAergic network activity is sufficient to precipitate generalized convulsive seizures, with a portion of these events leading to death in Gad2-*Ndufs4*-KO mice, but not in control mice. These findings suggest that careful avoidance of exogenous factors that suppress GABAergic network activity can help improve the efficacy of seizure management in LS. Furthermore, inclusion of agents that enhance activity in the same network may be beneficial for seizure prevention in LS. The association of mortality with a portion of PTZ-induced seizures may reflect the likelihood for a seizure to result in sudden death (sudden unexpected death, SUDEP) in LS.

Furthermore, our results show that mild exercise can act as a potent seizure trigger in our LS model. Exposure to mild exercise leads to convulsive seizures in Gad2-*Ndufs4*-KO mice (Fig. 1). The full mechanisms by which this exogenous factor precipitates seizures in our LS model remain unknown. Some human studies have shown that following exercise, there is an increase in brain metabolism in GABAergic interneurons (Maddock et al., 2016). Other studies in humans have revealed increases in cortical EEG power across delta and theta frequencies, following exercise (Crabbe and Dishman, 2004). Therefore, we postulate that *Ndufs4* KO-related mitochondrial functional impairment in our LS model may disrupt normal brain activity homeostasis following exercise and thereby precipitate seizures. Together our results from the seizure trigger tests suggest that preventing or minimizing exposure to these identified triggers may help reduce seizure incidence, increase quality of life, and prevent epilepsy related deaths in children suffering from LS-related epilepsy or other mitochondrial diseases.

4.2. Deletion of Ndufs4 in GABAergic interneurons leads to altered interneuron excitability

In the majority of interneurons, KO of *Ndufs4* resulted in a biphasic alteration in interneuron excitability marked by hyperactivity at low current injections followed by severe hypoactivity at higher current injections. These impaired mutant interneurons also showed a decrease in capacitance, rheobase, and AP height. Additionally, they showed an increase in AP width, input resistance, and afterhyperpolarization (AHP) (Fig. 2).

The hyperactivity of impaired mutant interneurons observed at lower depolarizations correlates with selected changes in cellular properties. The decrease in rheobase and capacitance may contribute to the increased firing of the interneuron. Reduced rheobase may be due to changes in ion channel expression or synaptic inputs, however, this remains to be investigated. Reduced capacitance may result from a reduction in cell surface area and ion

channel expression. Since hyperactivity of interneurons occurs at lower depolarizations, we hypothesize that it may contribute to network and EEG activity suppression during interictal periods.

Hypoexcitability at higher current injections is associated with increased input resistance. In addition, changes in three active membrane properties (decreased AP height and increased AP width and AHP) also align with the hypoactivity firing phenotype. The increase in input resistance suggests that membrane conductance and/or expression of an ion channel is reduced in these interneurons. We propose that hypoexcitability leads to an imbalance of excitation and inhibition in local networks, lowering the seizure threshold and precipitating seizures. Altered GABAergic interneuron function is a common characteristic of early-onset epileptic encephalopathies (Katsarou et al., 2017). Interneuron dysfunction promotes disinhibition in vulnerable brain regions laden with recurrent excitatory networks leading to network excitability, ictal events, and recurrent seizures. This has been specifically observed in the hippocampus where interneurons are known to be involved in seizure generation (Liautard et al., 2013; Jansen et al., 2020). Moreover, genetic models of early-life epilepsies reduce hippocampal interneuron excitability, without changing excitatory neuron activity, which is enough to cause disinhibition and spontaneous seizures (Yu et al., 2006; Katsarou et al., 2017). We have previously shown that targeted KO of *Ndufs4* to GABAergic interneurons is sufficient to produce spontaneous and provoked seizures in mice (Bolea et al., 2019). Thus LS-related epilepsy appears to be aligned with other early-life epileptic encephalopathies sharing altered GABAergic interneuron excitability as a pathophysiological mechanism. Together, our physiological recordings reveal that the *Ndufs4* KO alters interneuron function, providing a cellular mechanism of the severe seizure phenotype observed in LS. This observation suggests that restoration of the cellular properties via cell-specific gene therapy may be a potential therapeutic approach for treating epilepsy in mitochondrial diseases.

A smaller population of mutant interneurons (the unimpaired mutant group) did not reveal changes in excitability due to the *Ndufs4* KO. These unimpaired mutant interneurons showed the following minor changes in cellular properties: increase in AP height, AP width, and AHP (Fig. 2). These changes were not sufficient to alter excitability suggesting developmental mechanisms may influence pathophysiological mechanisms of mitochondrial disease epilepsies. Electrophysiological recordings of interneurons were sampled from P30–40 Gad2-*Ndufs4*-KO mice, an age before spontaneous seizures typically dominate the clinical phenotype (which occurs close to P55–60). The two distinct profiles (i. e., impaired vs unimpaired) of mutant interneurons may be the reflection of progression in the disease pathophysiological features. Further, since seizures themselves can accelerate an energy deficit (Wesół-Kucharska et al., 2021), it is possible that the interneuron functional deficit worsens at a later stage of development and when seizures are present. Therefore, a critical threshold of the percentage of interneuron population with a functional deficit may be necessary to offset the balance of excitation and inhibition, leading to spontaneous seizures. Future studies that record from interneurons across multiple developmental time points will be necessary to determine whether interneuron dysfunction, due to the *Ndufs4* KO, evolves/progresses over time.

Interestingly, a recent study of the 4-aminopyridine model of acute seizures, in the mouse entorhinal cortex in vitro, has shown that GABAergic interneurons (of all subtypes) play a key role in seizure initiation (Scalmani et al., 2023). However, this study reports that seizure onset is marked by a characteristic increase in firing of interneurons, followed by the recruitment of pyramidal neurons in this model. This observation is not consistent with the proposed mechanism of seizure initiation described above for our model. The authors argued that though they saw a loss of interneuron firing through depolarization block, this event did not coincide with seizure onset and was observed in a fraction of both excitatory and inhibitory neurons in their study. Therefore, they concluded that suppression of interneuron firing is unlikely to contribute to seizure initiation in their model. It is possible that the role of interneurons at seizure initiation is different in the two models. In the colleagues' model, interneurons are functionally unaltered before the application of the seizure trigger. In contrast, we showed that the interneurons are already functionally impaired due to the genetic mutation even before seizure test. Future electrophysiological studies in our model will shed more light on this question.

4.3. Deletion of Ndufs4 in GABAergic interneurons reduces interneuron cell density

KO of *Ndufs4* in GABAergic interneurons resulted in a nearly 30% reduction of interneurons across the CA1 hippocampus, central amygdala, and the posteromedial cortical amygdala nucleus (Fig. 3) with no change in cortical or other hippocampal regions (Supplementary Fig. 3). Reduced interneuron cell density in these regions shows that the *Ndufs4* KO in interneurons is sufficient to alter interneuron expression in key regions associated with epilepsy.

Interneuron cell loss was detected in CA1 hippocampus, a region commonly associated with epilepsy. Loss of inhibition, due to interneuron loss in the hippocampus, likely reduces network inhibition in this region and precipitates to seizures. Concurrent interneuron loss and dysfunction in the hippocampus likely leads to an excitatory and inhibitory imbalance and desynchronization of local networks (Maglóczky and Freund, 2005) lowering the seizure threshold. However, the mechanisms of interneuron loss remain unknown, and this is one limitation of this study. One possible mechanism is interneuron cell death which is a proposed mechanism of mitochondrial disease epilepsies (Wesół-Kucharska et al., 2021; Lopriore et al., 2022). Another possibility is impaired interneuron migration. The latter has been linked to dysfunction of mitochondria during neurodevelopment (Lin-Hendel et al., 2016). Future studies are necessary to determine the mechanisms of interneuron cell loss (i.e., necrosis, apoptosis, and impaired migration). In addition to interneuron loss, seizures trigger neuroinflammation in the hippocampus (Rizzi et al., 2003) increasing seizure susceptibility and risk of mortality (Somera-Molina et al., 2009). Extensive interneuron cell loss and gliosis occurs across the hippocampus including the CA1 subfield in other epilepsy syndromes (Thom, 2014; Rao et al., 2006). Future experiments will be necessary to determine the role of neuroinflammation in LS-related epilepsy.

Interneuron cell loss was also detected in the amygdala, a region implicated in dysfunctional breathing states during seizures (Lacuey et al., 2019; Nobis et al., 2019). Interestingly, seizures that have spread to the amygdala lead to a spontaneous breathing deficit in patients

with medically intractable epilepsy (Dlouhy et al., 2015). Since nearly all Gad2-*Ndufs4*-KO mice succumb to sudden unexpected death in epilepsy (SUDEP) (Bolea et al., 2019), it is possible that dysfunctional activity in the amygdala drives the SUDEP phenotype in LS epilepsy. Future studies investigating the mechanisms of SUDEP in these mice may lead to novel treatments that prevent premature death in mitochondrial-related epilepsies.

Surprisingly, cell loss was not detected in the cortex in Gad2-*Ndufs4*-KO mice. The cortex is commonly implicated in driving epilepsy. The epilepsy component in LS often varies in onset, progression, and severity (Finsterer and Mahjoub, 2012), making the clinical course and disease prognosis of each patient different (Yoshinaga et al., 1993). Further, models of LS, including the Gad2-*Ndufs4*-KO model, recapitulate variable disease presentation, where epilepsy onset, progression, and severity is slightly different for each animal. Thus, no cell loss across different cortical regions may be due to varied seizure histories across the mutant cohort. Therefore, tracking the entire seizure history alongside interneuron expression changes will be critical to understanding the relationship between cortical interneuron expression changes and the epilepsy phenotype. Alternatively, it is possible that interneurons in the cortex are not as vulnerable to interneuron loss compared to interneurons in the hippocampus and other regions. Finally, while cortical interneurons may not be susceptible to interneuron loss, the *Ndufs4* KO may be sufficient to alter excitability in these cells. Further studies will be necessary to assess the impact of the *Ndufs4* KO on cortical interneuron excitability.

Together, these experiments revealed that targeted *Ndufs4* KO to GABAergic interneurons causes reduced interneuron cell density in the hippocampus and amygdala. Interestingly, reduced interneuron cell density correlates with spontaneous, convulsive seizures, and premature death associated with seizures in Gad2-*Ndufs4*-KO mice. Further, concurrent loss and dysfunction and of these interneurons in CA1 hippocampus likely allows excitation to go unchecked, which may drive the spontaneous seizure phenotype previously described in the Gad2-*Ndufs4*-KO model (Bolea et al., 2019).

4.4. Cfos expression reveals the hippocampus and cortex are involved in seizure activity in Gad2-Ndufs4-KO mice

Following thermally-induced and spontaneous GTC seizures, Gad2-*Ndufs4*-KO mice exhibited an increase in cFos expression in the dentate gyrus (DG) of the hippocampus and the frontal cortex (Fig. 4).

The DG is thought to serve as a “gate”, protecting the hippocampal circuitry from overexcitation. When it is compromised, excess activity is likely to occur in the hippocampus, spreads to other downstream brain areas, and results in seizures (Heinemann et al., 1992; Lothman et al., 1992; Krook-Magnuson et al., 2015). Additionally, cortical engagement has been previously described in animal models of epilepsy (Tai et al., 2014; Katsarou et al., 2017). Accordingly, our cfos results demonstrate that the DG and cortex are involved in seizure generation in these mice. Further, our results reflect the fact that GTC seizures involve multiple brain regions. Thermally induced and spontaneous GTC seizures both lead to a similar pattern of cFos activity in the hippocampus and prefrontal cortex. However, it is worth noting that only one mouse exhibited a spontaneous seizure in our

experiments. Future experiments will investigate in depth whether seizures induced via the three different methods (namely thermal, PTZ, and exercise seizure tests) used this study will lead to the same cfos expression profile.

Hippocampus and frontal cortex have been shown to be implicated in the generation of seizures in several animal models of PTZ-epilepsy. Studies of rats, marmosets, and monkeys subjected to PTZ showed seizures followed by transient cFos activation in the DG and medial prefrontal cortex (mPFC) (Barros et al., 2015; Yang et al., 2019). Work in rodents have shown increased cFos activity in the prefrontal cortex following PTZ-induced seizures (Szyndler et al., 2009). Therefore, these previous research findings suggest that seizures evoked by elevation of temperature or PTZ may activate the same brain regions in our mouse model of LS. But, whether exercise-induced seizures will lead to the same physiological response is not hard to predict based on available information.

5. Conclusions

Taken together, our data provide an important insight into the mechanisms of LS epilepsy. They indicate that a LS-causing mutation mainly leads to a significant decrease in interneuron density and impaired excitability of remaining interneurons. In turn, these neuroanatomical and functional changes result in hyperexcitability of neuronal populations in the hippocampus and cortex, along with increased susceptibility to spontaneous and evoked seizures. Since the studied mutation is known to compromise mitochondrial function via suppression of complex I expression (Kruse et al., 2008), we predict that similar mechanisms may underlie the pathogenesis of epilepsy in other forms of mitochondrial diseases.

Several pathophysiological mechanisms underlying epilepsy in mitochondrial diseases have been previously hypothesized. Our findings in this study are aligned with the hypothesis that mitochondrial dysfunction leads to reduced interneuron activity and/or interneuron cell loss, leading to an imbalance of excitation and inhibition, and resulting in seizures. A limitation of this part of our study is that our experiments did not assess other hypotheses, namely that mitochondrial dysfunction leads to (1) abnormal ion channel expression/function; (2) impaired Na^+/K^+ ATPase activity; (3) impaired calcium homeostasis; or (4) the generation of reactive oxygen species (ROS) (Wesół-Kucharska et al., 2021; Lopriore et al., 2022). These mechanisms can also lead to network hyperactivity and seizures. However, our work suggests that the hypothesis that mitochondrial dysfunction leads to increased excitability in glutamatergic neurons which translate into seizures may not apply to our model given that the *Ndufs4* mutation was not introduced in this cell type.

Different interneuron subtypes are thought to have differential vulnerabilities to mitochondrial dysfunctions due to their distinct electrophysiological properties and associated energy demands. It is therefore conceivable that interneuron subtypes play differential roles in mechanisms of epilepsy in LS or other mitochondrial diseases. However, this hypothesis was not tested in this study. But our future study will investigate the relative contribution of the two main interneuron subtypes, parvalbumin (PV) and somatostatin (SST), to the epileptic phenotype in our LS model. Interestingly, impaired PV interneuron

excitability is known to alter the balance of excitation and inhibition leading to spontaneous seizures in models of early-onset epileptic encephalopathies (Rubinstein et al., 2015; Inan et al., 2016; Piguet et al., 2018; Joseph et al., 2020). On the other end, impaired SST interneuron excitability only produces a mild epileptic phenotype (Rubinstein et al., 2015). Understanding the roles of interneuron subtypes in the mechanisms of epilepsy in mitochondrial disease will help in the development of highly precise therapies for this disease.

Supplementary Material

Refer to Web version on PubMed Central for supplementary material.

Acknowledgements

The authors thank Dr. Aguan Wei from Seattle Children's Research Institute for his insightful and constructive input on the writing of the manuscript.

Funding statement

Research reported in this publication was supported by the National Institute of Neurological Disorders and Stroke (NINDS) of the National Institute of Health (NIH) (F31NS118991 to A.M.) (R01 NS102796 to F·K.).

Data availability

Data will be made available on request.

References

Arii J, Tanabe Y, 2000. Leigh syndrome: serial MR imaging and clinical follow-up. AJNR Am. J. Neuroradiol 21 (8), 1502–1509. Retrieved from (in place of doi): https://www.ajnr.org/content/21/8/1502.long. [PubMed: 11003287]

Balamurugan E, et al. , 2013. Perceived trigger factors of seizures in persons with epilepsy. Seizure 22 (9), 743–747. 10.1016/j.seizure.2013.05.018. [PubMed: 23806632]

Barros Vanessa N., et al. , 12 Mar 2015. The pattern of c-Fos expression and its refractory period in the brain of rats and monkeys. Front. Cell. Neurosci 9, 72. 10.3389/fncel.2015.00072. [PubMed: 25814929]

Bolea Irene, et al. , 12 Aug 2019. Defined neuronal populations drive fatal phenotype in a mouse model of Leigh syndrome. eLife 8. 10.7554/eLife.47163 e47163. [PubMed: 31403401]

Bornstein Rebecca, et al. , 2022. Differential effects of mTOR inhibition and dietary ketosis in a mouse model of subacute necrotizing encephalomyelopathy. Neurobiol. Dis 163, 105594. 10.1016/j.nbd.2021.105594. [PubMed: 34933094]

Bris Celine, et al. , 11 Dec 2017. Novel *NDUFS4* gene mutation in an atypical late-onset mitochondrial form of multifocal dystonia. Neurol. Genet 3 (6) 10.1212/NXG.0000000000000205 e205. [PubMed: 29264396]

Calvaruso Maria Antonietta, et al. , 2012. Mitochondrial complex III stabilizes complex I in the absence of NDUFS4 to provide partial activity. Hum. Mol. Genet 21 (1), 115–120. 10.1093/hmg/ddr446. [PubMed: 21965299]

Crabbe James B., Dishman Rod K., 2004. Brain electrocortical activity during and after exercise: a quantitative synthesis. Psychophysiology 41 (4), 563–574. 10.1111/j.1469-8986.2004.00176.x. [PubMed: 15189479]

Dlouhy Brian J., et al. , 2015. Breathing inhibited when seizures spread to the amygdala and upon amygdala stimulation. J. Neurosci 35 (28), 10281–10289. 10.1523/JNEUROSCI.0888-15.2015. [PubMed: 26180203]

Eloqayli H, et al. , 2003. Pentylenetetrazole decreases metabolic glutamate turnover in rat brain. J Neurochem 85, 1200–1207. 10.1046/j.1471-4159.2003.01781.x. [PubMed: 12753079]

Erakovic V, et al. , 2001. Altered activities of rat brain metabolic enzymes caused by pentylenetetrazol kindling and pentylenetetrazol–induced seizures. Epilepsy Res 43, 165–173. 10.1016/s0920-1211(00)00197-2. [PubMed: 11164705]

Finsterer Josef, Mahjoub Sinda Zarrouk, 2012. Epilepsy in mitochondrial disorders. Seizure 21 (5), 316–321. 10.1016/j.seizure.2012.03.003. [PubMed: 22459315]

Franklin KBJ, Paxinos G, 2013. Paxinos and Franklin's The mouse brain in stereotaxic coordinates. Academic Press, an imprint of Elsevier, Amsterdam.

Ge Anjie, et al. , 2022. Seizure triggers identified postictally using a smart watch reporting system. Epilepsy Behav. 126, 108472. 10.1016/j.yebeh.2021.108472. [PubMed: 34942507]

Heinemann U, et al. , 1992. The dentate gyrus as a regulated gate for the propagation of epileptiform activity. Epilepsy Res. Suppl 7, 273–280. [PubMed: 1334666]

Herrera DG, Robertson HA, 1996. Activation of c-fos in the brain. Prog. Neurobiol 50 (2–3), 83–107. 10.1016/s0301-0082(96)00021-4. [PubMed: 8971979]

Hunt Robert F., Baraban Scott C., 1 Dec 2015. Interneuron transplantation as a treatment for epilepsy. Cold Spring Harbor Perspect. Med 5 (12) 10.1101/cshperspect.a022376 a022376.

Inan Melis, et al. , 2016. Energy deficit in parvalbumin neurons leads to circuit dysfunction, impaired sensory gating and social disability. Neurobiol. Dis 93, 35–46. 10.1016/j.nbd.2016.04.004. [PubMed: 27105708]

Jansen Nico A., et al. , 2020. Focal and generalized seizure activity after local hippocampal or cortical ablation of Na_V 1.1 channels in mice. Epilepsia 61 (4), e30–e36. 10.1111/epi.16482. [PubMed: 32190912]

Joseph Donald J., et al. , 28 Dec 2020. Postnatal *Arx* transcriptional activity regulates functional properties of PV interneurons. iScience 24 (1), 101999. 10.1016/j.isci.2020.101999. [PubMed: 33490907]

Kang Hoon-Chul, et al. , 2013. Mitochondrial disease and epilepsy. Brain Dev. 35 (8), 757–761. 10.1016/j.braindev.2013.01.006. [PubMed: 23414619]

Kann Oliver, et al. , 2011. Gamma oscillations in the hippocampus require high complex I gene expression and strong functional performance of mitochondria. Brain 134 (Pt 2), 345–358. 10.1093/brain/awq333. [PubMed: 21183487]

Katsarou Anna-Maria, et al. , 2017. Interneuronopathies and their role in early LIFE epilepsies and neurodevelopmental disorders. Epilepsia Open 2 (3), 284–306. 10.1002/epi4.12062. [PubMed: 29062978]

Krall RL, et al. , 1978. Antiepileptic drug development: II. Anticonvulsant drug screening. Epilepsia 19 (4), 409–428. 10.1111/j.1528-1157.1978.tb04507.x. [PubMed: 699894]

Krook-Magnuson Esther, et al. , 2015. In vivo evaluation of the dentate gate theory in epilepsy. J. Physiol 593 (10), 2379–2388. 10.1113/JP270056. [PubMed: 25752305]

Kruse Shane E., et al. , 2008. Mice with mitochondrial complex I deficiency develop a fatal encephalomyopathy. Cell Metab. 7 (4), 312–320. 10.1016/j.cmet.2008.02.004. [PubMed: 18396137]

Lacuey Nuria, et al. , 2019. Limbic and paralimbic structures driving ictal central apnea. Neurology 92 (7), e655–e669. 10.1212/WNL.0000000000006920. [PubMed: 30635481]

Lake Nicole J., et al. , 2016. Leigh syndrome: one disorder, more than 75 monogenic causes. Ann. Neurol 79 (2), 190–203. 10.1002/ana.24551. [PubMed: 26506407]

Lax Nichola Z., et al. , 2016. Extensive respiratory chain defects in inhibitory interneurones in patients with mitochondrial disease. Neuropathol. Appl. Neurobiol 42 (2), 180–193. 10.1111/nan.12238. [PubMed: 25786813]

Lee Hsiu-Fen, et al. , 2009. Leigh syndrome: clinical and neuroimaging follow-up. Pediatr. Neurol 40 (2), 88–93. 10.1016/j.pediatrneurol.2008.09.020. [PubMed: 19135620]

Liautard Camille, et al. , 2013. Hippocampal hyperexcitability and specific epileptiform activity in a mouse model of Dravet syndrome. Epilepsia 54 (7), 1251–1261. 10.1111/epi.12213. [PubMed: 23663038]

Lin-Hendel EG, et al. , 2016. Differential Mitochondrial Requirements for Radially and Non-radially Migrating Cortical Neurons: Implications for Mitochondrial Disorders. Cell Rep 15, 229–237. 10.1016/j.celrep.2016.03.024. [PubMed: 27050514]

Lopriore Piervito, et al. , 2022. Mitochondrial epilepsy, a challenge for neurologists. Int. J. Mol. Sci 23 (21), 13216. 10.3390/ijms232113216. [PubMed: 36362003]

Löscher Wolfgang, 2017. Animal models of seizures and epilepsy: past, present, and future role for the discovery of Antiseizure drugs. Neurochem. Res 42 (7), 1873–1888. 10.1007/s11064-017-2222-z. [PubMed: 28290134]

Lothman EW, et al. , 1992. The dentate gyrus as a control point for seizures in the hippocampus and beyond. Epilepsy Res. Suppl 7, 301–313. [PubMed: 1334669]

Maddock Richard J., et al. , 2016. Acute modulation of cortical glutamate and GABA content by physical activity. J. Neurosci 36 (8), 2449–2457. 10.1523/JNEUROSCI.3455-15.2016. [PubMed: 26911692]

Maglóczky Zsófia, Freund Tamás F., 2005. Impaired and repaired inhibitory circuits in the epileptic human hippocampus. Trends Neurosci. 28 (6), 334–340. 10.1016/j.tins.2005.04.002. [PubMed: 15927690]

Morgan JI, et al. , 1987. Mapping patterns of c-fos expression in the central nervous system after seizure. Science (New York, N.Y.) 237 (4811), 192–197. 10.1126/science.3037702. [PubMed: 3037702]

Naess Karin, et al. , 2009. MtDNA mutations are a common cause of severe disease phenotypes in children with Leigh syndrome. Biochim. Biophys. Acta 1787 (5), 484–490. 10.1016/j.bbabio.2008.11.014. [PubMed: 19103152]

Nobis William P., et al. , 5 Apr 2019. The effect of seizure spread to the amygdala on respiration and onset of ictal central apnea. J. Neurosurg 132 (5), 1313–1323. 10.3171/2019.1.JNS183157. [PubMed: 30952127]

Oakley John C., et al. , 2009. Temperature- and age-dependent seizures in a mouse model of severe myoclonic epilepsy in infancy. Proc. Natl. Acad. Sci. U. S. A 106 (10), 3994–3999. 10.1073/pnas.0813330106. [PubMed: 19234123]

Ortigoza-Escobar Juan Darío, et al. , 2016. Ndufs4 related Leigh syndrome: a case report and review of the literature. Mitochondrion 28, 73–78. 10.1016/j.mito.2016.04.001. [PubMed: 27079373]

Piao Yue-Shan, et al. , 2006. Clinico-neuropathological study of a Chinese case of familial adult Leigh syndrome. Neuropathology 26 (3), 218–221. 10.1111/j.1440-1789.2006.00686.x. [PubMed: 16771178]

Piguet Françoise, et al. , 2018. Rapid and complete reversal of sensory ataxia by gene therapy in a novel model of Friedreich Ataxia. Mol. Ther 26 (8), 1940–1952. 10.1016/j.ymthe.2018.05.006. [PubMed: 29853274]

Quintana Albert, et al. , 2010. Complex I deficiency due to loss of Ndufs4 in the brain results in progressive encephalopathy resembling Leigh syndrome. Proc. Natl. Acad. Sci. U. S. A 107 (24), 10996–11001. 10.1073/pnas.1006214107. [PubMed: 20534480]

Racine R, et al. , 1972. Modification of seizure activity by electrical stimulation. 3. Mechanisms. Electroencephalogr. Clin. Neurophysiol 32 (3), 295–299. 10.1016/0013-4694(72)90178-2. [PubMed: 4110398]

Rahman Shamima, Copeland William C., 2019. POLG-related disorders and their neurological manifestations. Nat. Rev. Neurol 15 (1), 40–52. 10.1038/s41582-018-0101-0. [PubMed: 30451971]

Rahman S, et al. , 1996. Leigh syndrome: clinical features and biochemical and DNA abnormalities. Ann. Neurol 39 (3), 343–351. 10.1002/ana.410390311. [PubMed: 8602753]

Rahman S, et al. , 2012. Mitochondrial disease and epilepsy. Dev. Med. Child Neurol 54 (5), 397–406. 10.1111/j.1469-8749.2011.04214.x. [PubMed: 22283595]

Rao Muddanna S., et al. , 2006. Hippocampal neurodegeneration, spontaneous seizures, and mossy fiber sprouting in the F344 rat model of temporal lobe epilepsy. J. Neurosci. Res 83 (6), 1088–1105. 10.1002/jnr.20802. [PubMed: 16493685]

Rizzi Massimo, et al. , 2003. Glia activation and cytokine increase in rat hippocampus by kainic acid-induced status epilepticus during postnatal development. Neurobiol. Dis 14 (3), 494–503. 10.1016/j.nbd.2003.08.001. [PubMed: 14678765]

Rubinstein Moran, et al. , 2015. Dissecting the phenotypes of Dravet syndrome by gene deletion. Brain 138 (Pt 8), 2219–2233. 10.1093/brain/awv142. [PubMed: 26017580]

Scalmani P, et al. , 2023. Involvement of GABAergic interneuron subtypes in 4-Aminopyridine-induced seizure-like events in mouse entorhinal cortex in vitro. J. Neurosci 43 (11), 1987–2001. 10.1523/JNEUROSCI.1190-22.2023. [PubMed: 36810229]

Smeitink J, et al. , 2001. Human NADH:ubiquinone oxidoreductase. J. Bioenerg. Biomembr 33 (3), 259–266. 10.1023/a:1010743321800. [PubMed: 11695836]

Somera-Molina Kathleen C., et al. , 2009. Enhanced microglial activation and proinflammatory cytokine upregulation are linked to increased susceptibility to seizures and neurologic injury in a ‘two-hit’ seizure model. Brain Res. 1282, 162–172. 10.1016/j.brainres.2009.05.073. [PubMed: 19501063]

Szyndler Janusz, et al. , 2009. Mapping of c-Fos expression in the rat brain during the evolution of pentylenetetrazol-kindled seizures. Epilepsy Behav. 16 (2), 216–224. 10.1016/j.yebeh.2009.07.030. [PubMed: 19713157]

Tai Chao, et al. , 2014. Impaired excitability of somatostatin- and parvalbumin-expressing cortical interneurons in a mouse model of Dravet syndrome. Proc. Natl. Acad. Sci. U. S. A 111 (30), E3139–E3148. 10.1073/pnas.1411131111. [PubMed: 25024183]

Taniguchi Hiroki, et al. , 2011. A resource of Cre driver lines for genetic targeting of GABAergic neurons in cerebral cortex. Neuron 71 (6), 995–1013. 10.1016/j.neuron.2011.07.026. [PubMed: 21943598]

Thom Maria, 2014. Review: hippocampal sclerosis in epilepsy: a neuropathology review. Neuropathol. Appl. Neurobiol 40 (5), 520–543. 10.1111/nan.12150. [PubMed: 24762203]

Van Erum Jan, et al. , 2020. Pentylenetetrazole-induced seizure susceptibility in the Tau58/4 transgenic mouse model of Tauopathy. Neuroscience 425, 112–122. 10.1016/j.neuroscience.2019.11.007. [PubMed: 31785360]

van de Wal Melissa A.E., et al. , 2022. Ndufs4 knockout mouse models of Leigh syndrome: pathophysiology and intervention. Brain 145 (1), 45–63. 10.1093/brain/awab426. [PubMed: 34849584]

Wesół-Kucharska Dorota, et al. , 22 Jun 2021. Epilepsy in mitochondrial diseases-current state of knowledge on aetiology and treatment. Children (Basel, Switzerland) 8 (7), 532. 10.3390/children8070532. [PubMed: 34206602]

Whittaker Roger G., et al. , 2011. Impaired mitochondrial function abolishes gamma oscillations in the hippocampus through an effect on fast-spiking interneurons. Brain 134 (Pt 7). 10.1093/brain/awr018 e180; author reply e181. [PubMed: 21378098]

Yang Huajun, et al. , 2019. C-Fos mapping and EEG characteristics of multiple mice brain regions in pentylenetetrazol-induced seizure mice model. Neurol. Res 41 (8), 749–761. 10.1080/01616412.2019.1610839. [PubMed: 31038018]

Yoshinaga H, et al. , 1993. A T-to-G mutation at nucleotide pair 8993 in mitochondrial DNA in a patient with Leigh’s syndrome. J. Child Neurol 8 (2), 129–133. 10.1177/088307389300800204. [PubMed: 8505474]

Yu Frank H., et al. , 2006. Reduced sodium current in GABAergic interneurons in a mouse model of severe myoclonic epilepsy in infancy. Nat. Neurosci 9 (9), 1142–1149. 10.1038/nn1754. [PubMed: 16921370]

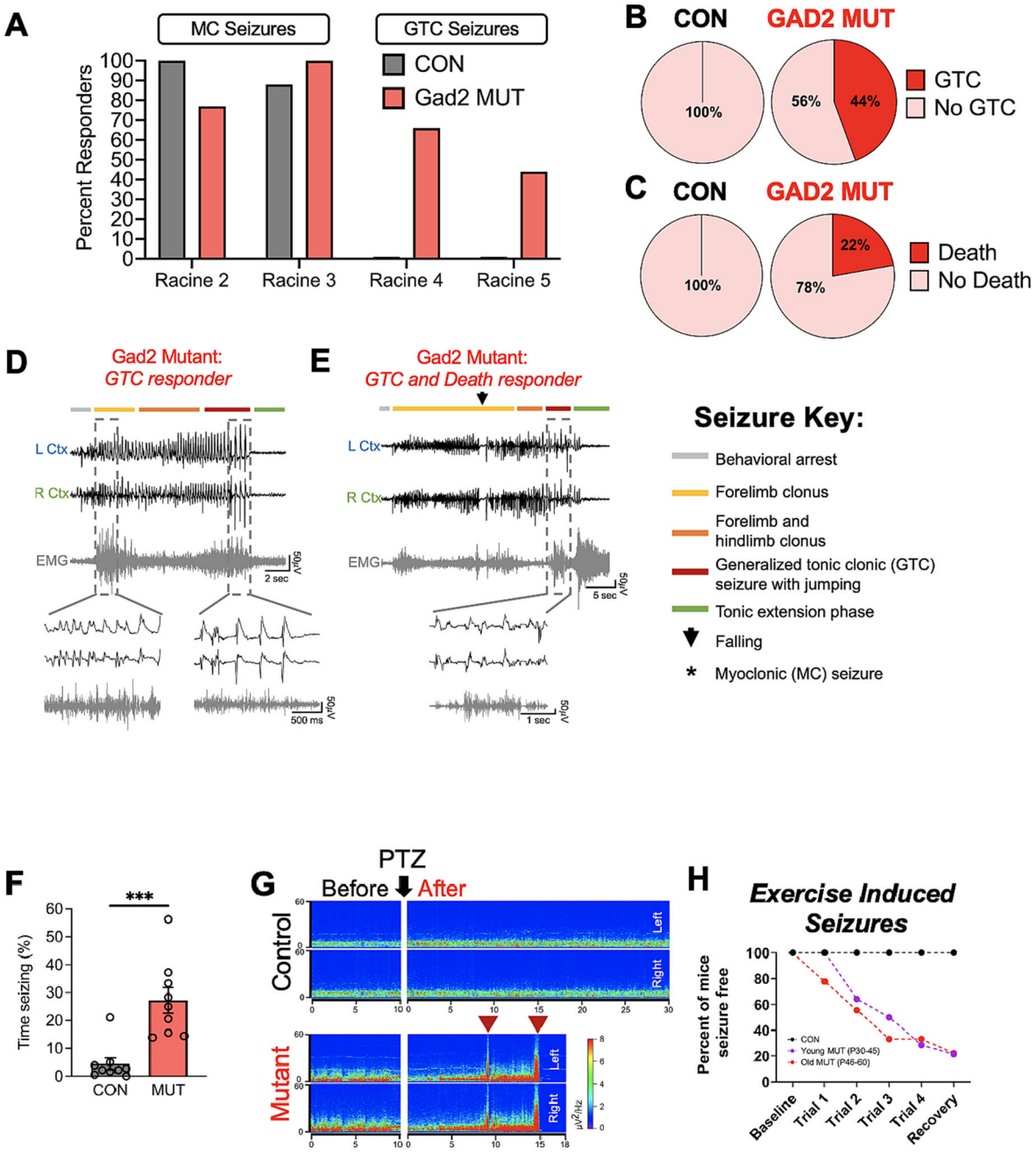

Fig. 1. Gad2-Ndufs4-KO mutants show a severe provoked seizure phenotype.

(A) 7–8-week-old GAD2 MUT mice showed greater susceptibility to PTZ-induced Racine 3–5 seizures than CON mice. (B) GAD2 MUT and CON percent responders for GTC seizures (Racine 4–5) and (C) death immediately following GTC seizures. (D) Representative EEG-EMG traces showing a severe GTC seizure in a mutant, and (E) severe GTC seizure followed by death in a different mutant (F)Mutants showed greater percent time in Racine 3–5 seizures compared to controls. (G) Heat map of EEG power spectra showing left and right hemisphere EEG activity at different frequencies (Hz) as a function

of time (minutes) from a representative control (top) and mutant (bottom) mouse before and after PTZ challenge. Mutant mouse showed two GTC seizures (red arrowheads) indicated by increased power activity prior to sudden death. GAD2 MUT: $N = 9$; CON: N = 9 and mouse age: P50–63, for PTZ experiments. (H) Kaplan-Meier curves estimating seizure susceptibility in GAD2 MUT mice exposed to a moderate exercise on the treadmill. The challenge consisted of four consecutive trials. Both young (P30–45) and old (P46–60) mutant mice showed seizure susceptibility. GAD2 MUT (Young): $N = 14$; GAD2 MUT (Old): N = 9; CON: $N = 12$. (For interpretation of the references to colour in this figure legend, the reader is referred to the web version of this article.)

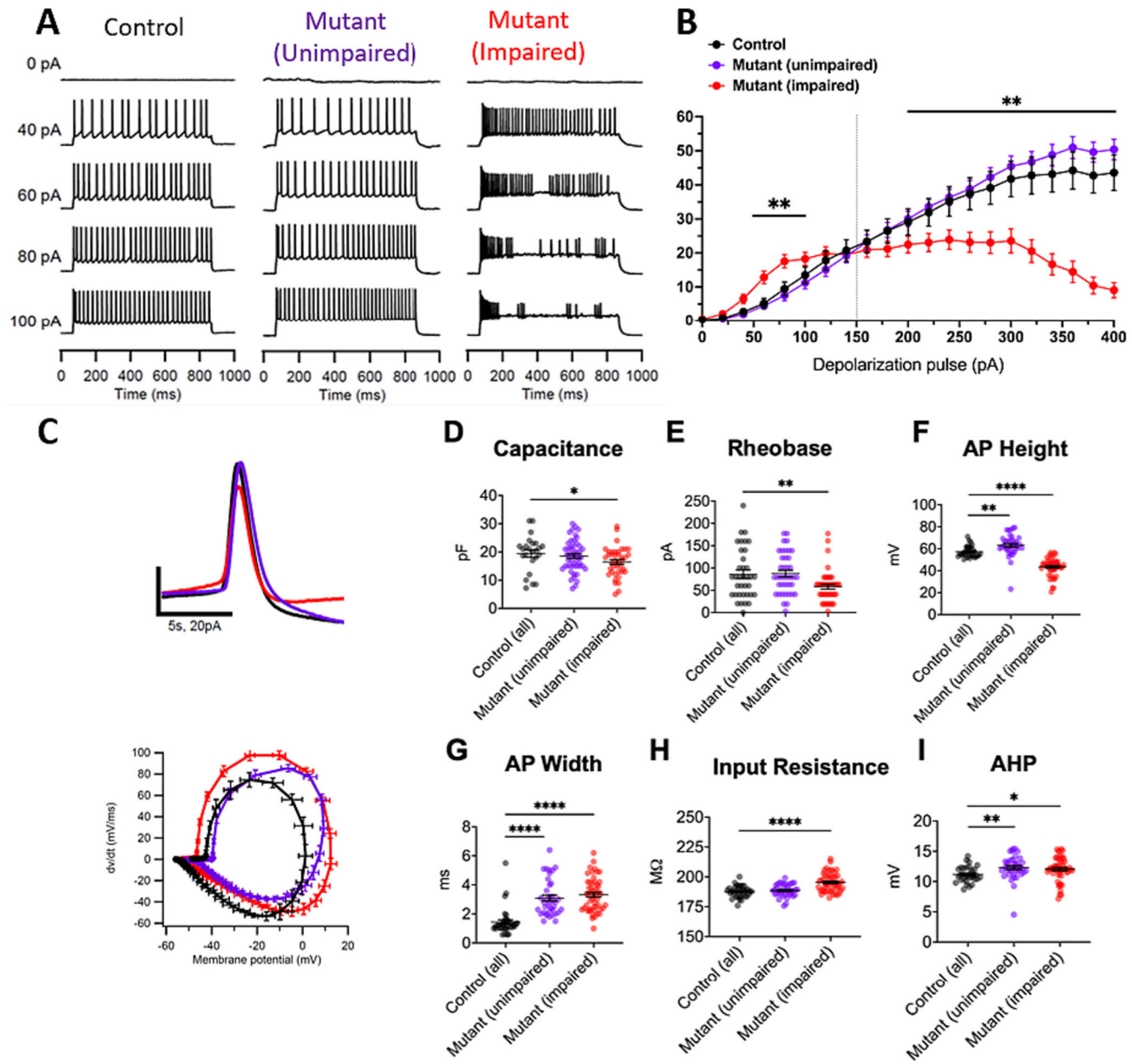

Fig. 2. Gad2-Ndufs4-KO mutants show impaired GABAergic interneuron firing.

(A) Sample traces of whole-cell current clamp recordings of hippocampal interneurons in response to increasing current injections. (B) Number of action potentials (APs) (mean±SEM) in response to 800 ms long depolarizing current injection at indicated intensities. Control number of cells (n = 36), Mutant impaired Group (n = 54), and Mutant unimpaired Group (n = 36) (C) *Top:* Examples of single AP traces recorded from interneurons of each group. *Bottom:* Average phase plots illustrating the first derivative of membrane potential as a function of membrane potential during action potential generation. The plots reveal differences in action potential dynamic across cell groups. Control (black); mutant impaired (red). (D) Mutant impaired cells showed a decrease in membrane

capacitance, (E) a decrease in rheobase. (F) Mutant unimpaired cells showed an increase, while mutant impaired cells showed a decrease in AP height. (G) Mutant unimpaired and impaired cells showed an increase in AP width. (H) Mutant impaired cells showed an increase in input resistance. (I) Mutant unimpaired and impaired cells showed an increase in AHP. Control and mutant mice were P30–40. Data represents mean ± SEM and individual data points overlaid. (For interpretation of the references to colour in this figure legend, the reader is referred to the web version of this article.)

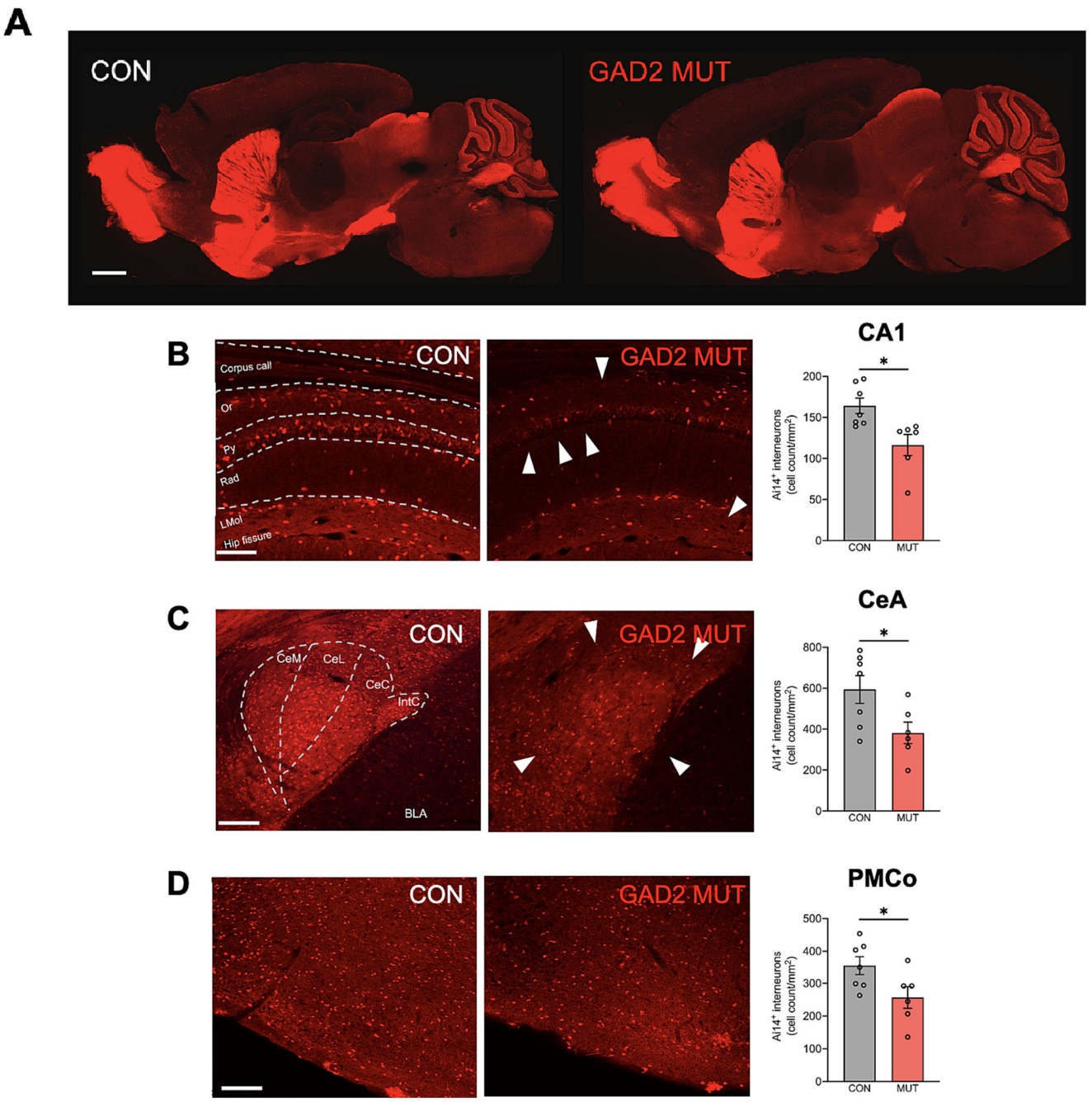

Fig. 3.

Gad2-Ndufs4-KO mice show interneuron loss in key regions associated with epilepsy. (A) Representative sagittal whole brain images from a CON (left) and GAD MUT (right) mouse. Ai14-labeled (tdTomato) GABAergic interneurons (scale bar: 1 mm). ((B) Cell loss analysis of hippocampal CA1 (caudal) region revealed a 30% decrease of Ai14-labeled interneuron cell density in GAD2 MUT mice (scale bar: 100 μm). (C) GAD2 MUT mice showed a 35% decrease in interneuron cell density in the central amygdala (CeA) (D) GAD2 MUT mice showed a 27% decrease in interneuron cell density in the posteromedial cortical amygdala

nucleus (PMCo). White arrow heads indicate where the most cell loss occurred. Mice were P43-50, GAD2 MUT: N = 6; CON: N = 7. Bar graphs (mean ± SEM).

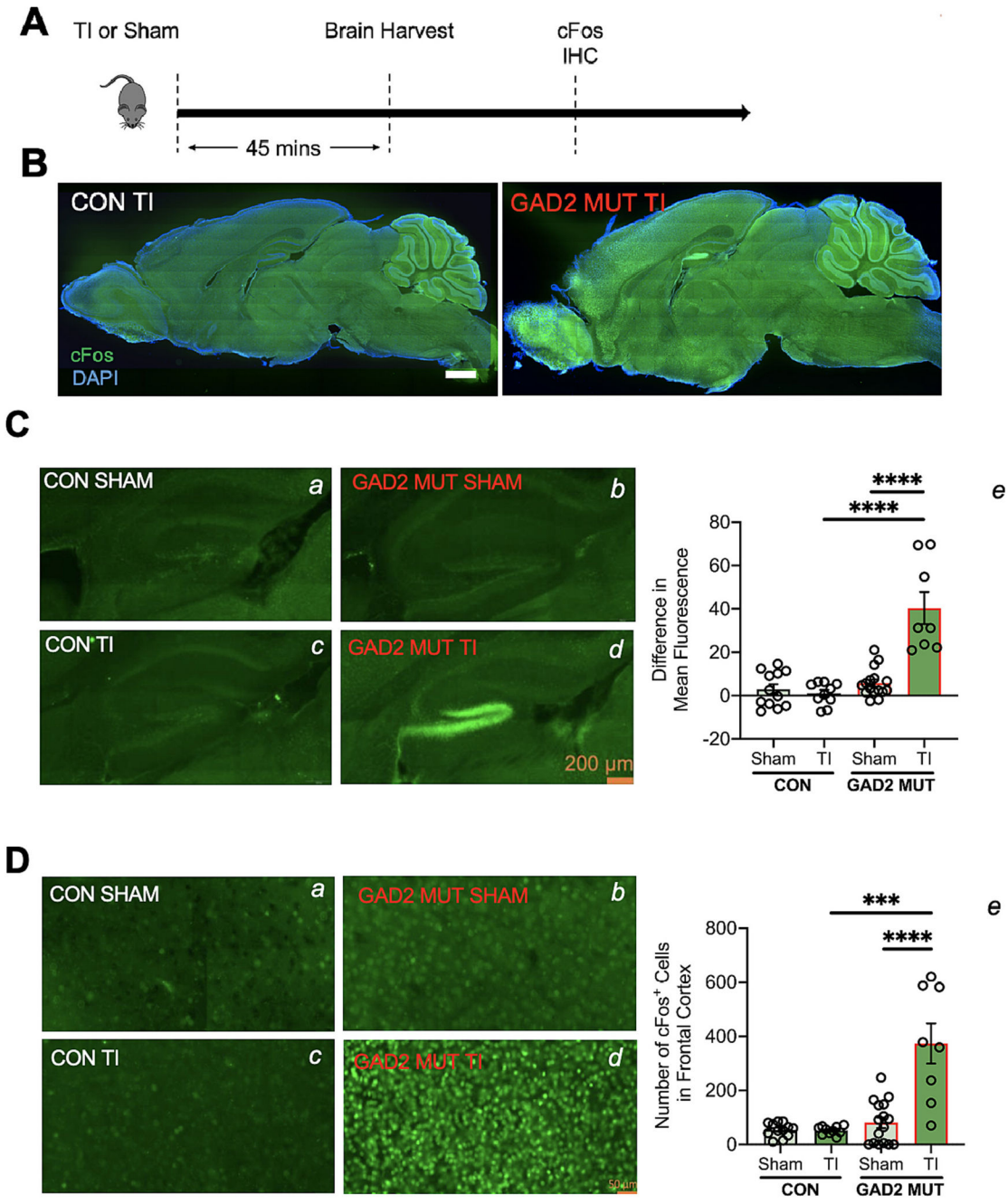

Fig. 4. Gad2-Ndufs4-KO mice show increased neuronal activity in key regions associated with epilepsy.

(A) Behavioral and histochemical paradigm. (B) Sagittal whole brain images of all groups (scale bar: 1 mm). (C) GAD2 MUT TI mice that displayed severe GTCs showed an increase in the difference in cFos mean fluorescence in the dentate gyrus (DG) of the hippocampus (scale bar: 200μm). (D) GAD2 MUT TI mice showed an increase in the number of cFos positive cells in the frontal cortex (scale bar:50μm). Mice were P55–60, GAD2 MUT sham:

$N = 8$, GAD2 MUT TI: $N = 7$, CON sham: $N = 6$, CON TI: $N = 5$. Each data point represents single mount (2 mounts per mouse). Bar graphs (mean±SEM).

Table 1

Electrophysiological parameters of CA1 interneurons in the hippocampus.

For parameter definitions, see Methods. Values are expressed as mean ± SEM.

	n		Intrinsic Properties							
Group	**Mice**	**Cells**	**V_m (mV)**	**C_m (pF)**	**Rheobase (pA)**	**Input Resistance (MΩ)**	**AP Height (mV)**	**AP Width (ms)**	**Threshold (#) (mV)**	**AHP (mV)**
Control	5	24	−57.0±1.7	19.4±1.3	81.7±9.3	187.5±0.8	57.1±0.8	1.4±0.1	−33.7±0.7	11.1±0.2
Gad2-*Ndufs4*-KO *Unimpaired*	8	49	−56.8±1.0	18.5±0.7	87.6±7.2	188.5±0.8	63.0±1.6 **	3.0±0.2 ****	−31.8±0.8	12.2±0.3 **
Gad2-*Ndufs4*-KO *Impaired*	7	40	−57.5±1.1	16.4±0.8 *	57.7±5.1 **	195.3±1.0 ****	43.4±1.1 ****	3.3±0.1 ****	−34.9±0.6	12.0±0.2 *

Significant differences between CON and Ndufs4$^{flx/flx}$*Gad2Cre*$^{+/-}$ (Unimpaired) or Ndufs4$^{flx/flx}$*Gad2Cre*$^{+/-}$ (Impaired) are expressed as

* $P < 0.05$;

** $P < 0.01$;

**** $p < 0.0001$,

Unpaired two-sample Student *t*-test.

(#) Threshold was determined using the second derivative. It was identified as the voltage at the time when the second differential of the action potential (AP) reaches its peak.